SLAC – PUB – 3972
DPNU – 86 – 15
May 1986
T/E

THE STRANGE MESON RESONANCES OBSERVED IN THE REACTION $K^-p \to \bar{K}^\circ\pi^+\pi^-n$ AT 11 GeV/c*

D. ASTON,[a] N. AWAJI,[b] J. D'AMORE,[c] W. DUNWOODIE,[a] R. ENDORF,[c] K. FUJII,[b‡] H. HAYASHII,[b♭] S. IWATA,[b‡] W.B. JOHNSON,[a] R. KAJIKAWA,[b] P. KUNZ,[a] D.W.G.S. LEITH,[a] L. LEVINSON,[a♮] T. MATSUI,[b‡] B.T. MEADOWS,[c] A. MIYAMOTO,[b‡] M. NUSSBAUM,[c] H. OZAKI,[b] C.O. PAK,[b‡] B.N. RATCLIFF,[a] D. SCHULTZ,[a] S. SHAPIRO,[a] T. SHIMOMURA,[b] P.K. SINERVO,[a†] A. SUGIYAMA,[b] S. SUZUKI,[b] G. TARNOPOLSKY,[a♯] T. TAUCHI,[b‡] N. TOGE,[a] K. UKAI,[d] A. WAITE,[a¶] S. WILLIAMS[a§]

[a] *Stanford Linear Accelerator Center, Stanford University, Stanford, California 94305*

[b] *Department of Physics, Nagoya University, Furo-Cho, Chikusa-ku, Nagoya 464, Japan*

[c] *Department of Physics, University of Cincinnati, Cincinnati, Ohio 45221*

[d] *Institute for Nuclear Study, University of Tokyo, 3-2-1 Midori-cho, Tanashi-shi, Tokyo 188, Japan*

Submitted to *Nuclear Physics B*

---

* Work supported in part by the Department of Energy under contract No. DE-AC03-76SF00515, and the National Science Foundation under grant No. PHY82-09144, and the Japan U.S. Cooperative Research Project on High Energy Physics.

Present Addresses:
‡ Nat. Lab. for High Energy Physics, KEK, Oho-machi, Tsukuba, Ibaraki 305, Japan.
♭ Nara Women's University, Kitauoya-nishi-machi, Nara-shi, Nara 630, Japan.
♮ Weizmann Institute, Rehovot 76100, Israel.
† University of Pennsylvania, Philadelphia, Pennsylvania 19104, U.S.A.
♯ Hewlett-Packard Laboratories, 1501 Page Mill Road, Palo Alto, California 94304, U.S.A.
¶ Department of Physics, University of Victoria, Victoria BC, Canada V8W 2Y2
§ Diasonics Corp., 533 Cabot Rd., S. San Francisco, CA 94090, U.S.A.

ABSTRACT

A model incorporating K^* resonance contributions and simple backgrounds is shown to quantitatively reproduce the mass dependence of the partial wave amplitudes governing the production and decay of the $\bar{K}^\circ \pi^+\pi^-$ system. A fit of this model to these amplitudes confirms the resonance interpretations of the well-established 1^+ $K_1(1400)$, the 2^+ $K_2^*(1430)$, the 3^- $K_3^*(1780)$, and the less well-known 1^- states, the $K^*(1410)$ and the $K^*(1790)$. The 4^+ amplitudes are shown to be consistent with the production and decay of the 4^+ $K_4^*(2060)$. A second 2^+ enhancement at a mass of $\sim$1.95 GeV/c^2 can be interpreted as resonant and may be the radial excitation of the $K_2^*(1430)$ or the triplet partner of the $K_4^*(2060)$. New measurements of the masses, widths and branching ratios of these states are given, and the implications of these data for the spectroscopy of the nonstrange meson sector are discussed.

1. Introduction

The spectroscopy of the light-quark meson states in the 1-2 GeV/c^2 mass range plays a significant role in the ongoing investigations in elementary particle physics, both as a probe of the $q\bar{q}$ potential and for the insight a detailed knowledge of such spectra provides into the nature of unusual states that have been observed in this mass region. The strange mesons appear to be an ideal place to study $q\bar{q}$ spectroscopy; the absence of glueballs and isoscalar mixing makes the phenomenology of the strange mesons less complicated, the visible decay of the K°_s eases experimental access to states of any charge, and the states can be easily produced with high-energy kaon beams. The two-body $K\pi$ [1–3] and three-body $K\pi\pi$ [4–14] systems have been the best source of information on strange mesons, in both diffractive and charge-exchange reactions. However, the $K\pi$ system can yield information on natural spin-parity amplitudes only. In contrast, the diffractive production of the $K\pi\pi$ system is dominantly via unnatural spin-parity states, whereas the charge-exchange production of the three-body system is dominated by natural spin-parity amplitudes.

The present analysis makes use of data on the $\bar{K}^\circ\,\pi^+\pi^-$ system produced in the charge-exchange reaction $K^-p \rightarrow \bar{K}^\circ\,\pi^+\pi^-n$ at 11 GeV/c and detected in the LASS spectrometer. The sensitivity of the experiment is ~4 events/nb, and the data set used contains ~34 000 events with $m(\bar{K}^\circ\,\pi^+\pi^-) \leq 2.3$ GeV/c^2 and $|t'| \leq 0.3$ (GeV/c)^2; this sample is approximately five times larger than any previously studied.

A three-body Partial Wave Analysis (PWA) shows that more than two-thirds of the events in this kinematic region are resonantly produced and subsequently decay via quasi-two-body modes to the $\bar{K}^\circ\,\pi^+\pi^-$ final state; the production of

natural spin-parity states is predominant. The partial wave amplitudes obtained are parametrized in terms of Breit-Wigner resonances and simple backgrounds. The resulting fits yield measurements of the masses, widths, and branching fractions of the natural and unnatural spin-parity strange mesons that are produced against a recoil neutron.

The details of the experiment and the PWA can be found in ref. [15].

2. The $\bar{K}^\circ \pi^+\pi^-$ Partial Wave Amplitudes

The $\bar{K}^\circ \pi^+\pi^-$ invariant mass spectrum for the $\bar{K}^\circ \pi^+\pi^- n$ event sample is shown in fig. 1. There are clear peaks at $\sim$1.45 and $\sim$1.8 GeV/c^2 and there is perhaps a shoulder around 2 GeV/c^2 on top of a broad continuum of events. Despite the rather uncomplicated appearance of this spectrum, the partial wave analysis uncovers an underlying resonance structure that is quite complex. The spin-parity decomposition of the acceptance-corrected cross section is shown in fig. 2 where the contributions to partial wave amplitudes of the same J^P have been added coherently and the resulting intensity plotted as a function of $\bar{K}^\circ \pi^+\pi^-$ invariant mass. Clear resonance signals are seen for 2^+ $K_2^*(1430)$, 3^- $K_3^*(1780)$, and 1^+ $K_1(1400)$ production. The J^P=1^- cross section has a shoulder around 1.45 GeV/c^2 followed by a dramatic peak at $\sim$1.8 GeV/c^2, with the cross section falling rapidly above 2 GeV/c^2. The further decomposition into the different isobar partial waves shows that this structure results from the production and decay of two previously observed [14] 1^- states, one at $\sim$1.42 GeV/c^2 (the $K^*(1410)$) and the other at $\sim$1.74 GeV/c^2, which is identified as the $K^*(1790)$. At high mass, there is evidence for 4^+ $K_4^*(2060)$ production and decay. Finally, there is a bump in the 2^+ amplitude around 2 GeV/c^2 that may be resonant.

The parameters of these resonant states have been estimated by performing fits of resonance lineshapes and simple backgrounds to the $\bar{K}^\circ \pi^+\pi^-$ partial wave amplitudes. Consider the processes

$$K^- p \to \mathcal{R} n \to \; a_j \; b_j n, \tag{1}$$

where $\mathcal{R}$ is a resonant state that has k two-body decay modes $a_j b_j$, for $j = 1$ to k. The mass and total width of $\mathcal{R}$ are denoted by M_0 and Γ^{tot} and the partial widths of the k decay modes of $\mathcal{R}$ are given by Γ^j, $j = 1$ to k. The differential cross section for eq. (1) can be written as [16]

$$d\sigma_R^j = F \left[\frac{\sqrt{M_0 \Gamma^j}}{{M_0}^2 - M^2 - i M_0 \Gamma^{tot}} \right]^2 M dM. \tag{2}$$

Here, M is the invariant mass of the $a_j b_j$ system and, as is usual in physical region Breit-Wigner fitting, any M-dependence of the term F is neglected. The angular correlations in the final states are ignored as they are not relevant to the following discussion.

By definition, eq. (2) has the phase space dependence of the final state subsumed in the partial width Γ^j. The form of Γ^j used in this analysis is

$$\Gamma^j = \frac{\left(\gamma^j\right)^2 D_{L_j}(Q_j)}{M_0} \left(\frac{Q_j}{M} \right), \tag{3}$$

where Q_j is the 3-momentum of a_j (or b_j) in the rest frame of $\mathcal{R}$, and γ^j is called the reduced coupling [17] and is a constant independent of M and Q_j (γ^j has units of energy). The function $D_{L_j}(Q_j)$ is an angular momentum barrier factor normally included in the partial width [18] Note that the last factor in eq. (3)

accounts for the M and Q_j dependence of the $a_j b_j$ phase space. The total width, Γ^{tot}, of $\mathcal{R}$ is defined as

$$\begin{aligned}\Gamma^{tot} &= \sum_{j=1}^{k} \Gamma^j \\ &= \sum_{j=1}^{k} \frac{(\gamma^j)^2 D_{L_j}(Q_j)}{M_0} \left(\frac{Q_j}{M}\right).\end{aligned} \tag{4}$$

In the isobar model, the decay of $\mathcal{R}$ into the final three-body system is pictured as taking place first into $a_j b_j$, with a_j subsequently decaying into the two other mesons. In this context, M is the invariant three-meson mass M_3. Using eq. (2) to write down the probability for this decay chain, the differential cross section becomes

$$\begin{aligned}d\sigma &= F\left[\sqrt{\frac{Q_j q_j}{m}} \left(\frac{\gamma^j \sqrt{D_{L_j}(Q_j)}}{{M_0}^2 - M^2 - iM_0\Gamma^{tot}}\right) \left(\frac{\gamma_j^{iso}\sqrt{D_{l_j}(q_j)}}{m_j^2 - m^2 - im_j\Gamma_j^{iso}}\right)\right]^2 dM d^5\omega \\ &= \left[\left(\frac{\sqrt{F}\gamma^j}{{M_0}^2 - M^2 - iM_0\Gamma^{tot}}\right) \right. \\ &\qquad \left. \left(\sqrt{\frac{Q_j q_j}{m}} \frac{\gamma_j^{iso}\sqrt{D_{L_j}(Q_j) D_{l_j}(q_j)}}{m_j^2 - m^2 - im_j\Gamma_j^{iso}}\right)\right]^2 dM d^5\omega,\end{aligned} \tag{5}$$

where m_0 and Γ_j^{iso} are the central mass and width of a_j, m is its two-body invariant mass, and q_j is the 3-momentum of one of the daughters of a_j in the a_j rest frame. The infinitesimal $d\omega^5$ is $dm^2 d\cos\theta d\alpha d\cos\beta d\gamma$, the t channel helicity angle θ and the Euler angles α, β, and γ being defined for the a_j isobar.

Equation (5) is the form used to parametrize the resonance contributions of the partial wave intensities. It explicitly takes into account the phase space for the three-body final state, suitably modified by the presence of the isobar.

The intensities presented in ref. [15] correspond to the eight-fold differential cross section integrated over a trivial lab azimuthal angle, the five variables describing the isobar-bachelor system and the decay of the isobar, and the $|t'|$ interval from 0.0 to 0.3 $(\mathrm{GeV/c})^2$. Hence, the expression in eq. (5) is also integrated over these seven variables to produce the predicted $d\sigma/dM$ for a resonant state. The Partial Wave Analysis (PWA) gives the intensities and relative phases of the three-body partial wave amplitudes required to describe the $\bar{K}^\circ \pi^+\pi^-$ system up to a three-body invariant mass of 2.3 $\mathrm{GeV/c^2}$. The resonance contributions to these partial wave intensities are determined by performing simultaneous fits of Breit-Wigner lineshapes to the real and imaginary parts of the measured partial wave amplitudes.

The parameters describing the resonance lineshapes are estimated by minimizing a χ^2 function defined using the difference vector of the predicted and measured partial wave amplitudes and the full error matrix from the fit to the partial waves in each mass bin. The error matrices from the PWA reflect the statistical uncertainties and correlations of the amplitudes, but do not account for the additional uncertainties arising from other sources such as: (a) the exclusion of statistically insignificant partial waves from the fitted wave set; (b) the statistical errors in the Monte Carlo acceptance calculation; and (c) the approximations of the isobar model. The additional uncertainty from these sources has been estimated to be $\sim$30 events/(0.02 $\mathrm{GeV/c^2}$) and has been added in quadrature to the statistical error of each partial wave amplitude. Since the typical statistical uncertainty is of the order of 100 events/(0.02 $\mathrm{GeV/c^2}$), the inclusion of the additional systematic uncertainty has little effect on the parameters extracted from the χ^2 fits.

The program **MINUIT** [19] is used to minimize the χ^2 function. In the results that follow, the quoted statistical errors are those determined by **MINUIT** and are based on the numerical evaluation of the second derivative of the χ^2 function at its minimum. In cases where an additional error is quoted, it is a systematic uncertainty that reflects the sensitivity of the result to various assumptions, such as the form of the background parametrizations.

The quoted branching fractions are defined by the ratio of the partial widths evaluated at the resonance mass M_0 (to be consistent with the definition used by the Particle Data Group [20]). Explicitly, the partial width corresponding to the jth decay mode is obtained from eq. (5) as

$$\Gamma^j = \frac{\gamma_j^2}{M_0} \left\{ \int d\omega^5 \frac{Q_j q_j (\gamma_j^{iso})^2 D_{L_j}(Q_j) D_{l_j}(q_j)}{Mm \left[(m_j^2 - m^2)^2 + (m_j \Gamma_j^{iso})^2 \right]} \right\}_{M=M_0} ; \qquad (6)$$

and it follows from eq. (5) that branching ratios based on eq. (6) are equal to ratios of $d\sigma/dM$ evaluated at $M = M_0$.

For most resonances, this definition of the branching ratio differs from the ratio of total cross sections because of the difference in resonant lineshape for different decay modes (due primarily to the energy-dependence of the partial width). Differential and total cross sections are quoted for the $|t'|$ bin 0.0–0.3 (GeV/c)^2 unless explicitly stated otherwise, and when given in events/0.02 GeV/c^2 they have not been corrected for isospin or K_s° visibility. The sensitivity of this experiment is 4.082 events/nb, and the K_s° branching ratio to $\pi^+\pi^-$ is 0.3431 [21], so that the factor to convert acceptance-corrected events to μbarns in the $\bar{K}^\circ \pi^+\pi^- n$ final state is 7.141×10^{-4} in all cases.

3. Results

3.1 THE 1^+ $K_1(1400)$

The $1^+0^+K^*S$ [#1] intensity distribution given in fig. 3(a) shows a peak at ~1.4 GeV/c^2 that results from the production and decay of the axial-vector $K_1(1400)$. The lack of a similar effect in the $1^+0^+\rho S$ intensity is consistent with this interpretation, as the $K_1(1400)$ is known to have a very small $K\rho$ coupling [21].

The $1^+0^+K^*S$ intensity in the mass region between 1.11 and 1.75 GeV/c^2 was parametrized by a resonance lineshape with a quadratic background that had an arbitrary phase relative to the resonant term. The 1.07 GeV/c^2 mass bin, which is strongly affected by phase space, was not used in the fit to determine the $K_1(1400)$ parameters. Table 1 presents the results of the fit; the differential cross section is given for the peak of the resonance, and the quoted systematic errors reflect the sensitivity of the results to different background parametrizations.

The result of the fit is also shown in fig. 3(a) and provides an excellent description of the data. The values for the $K_1(1400)$ mass and width are in good agreement with earlier observations of this resonance in the diffractively produced three-body final states [7–12] and in $\bar{K}^\circ\,\pi^+\pi^-n$ [13].

[#1] Each partial wave amplitude is specified in the notation $J^PM^\eta(isobar)L$, where J^P and M are the spin-parity and magnetic quantum numbers of the state in question, which decays to a quasi-two-body state consisting of the *isobar* and bachelor mesons with relative orbital angular momentum L; η specifies the naturality of the exchanged system in the t-channel. For conciseness in specifying isobars and decay modes we use K^*, K_2^* and ρ to denote $K^*(892)$, $K_2^*(1430)$ and $\rho(770)$ respectively.

Table 1

The 1^+ $K_1(1400)$ parameters. The differential cross section is quoted at the peak of the resonance in events/(0.02 GeV/c^2).

$K_1(1400) \rightarrow 1^+0^+K^*S$	
Mass (GeV/c^2)	$1.373 \pm 0.014 \pm 0.018$
Width (GeV/c^2)	$0.188 \pm 0.054 \pm 0.060$
χ^2/DOF	7.4/7
$d\sigma/dM_3$	$545 \pm 48 \pm 18$

3.2 THE 2^+ $K_2^*(1430)$

The $2^+0^-K^*D$ and $2^+0^-\rho D$ partial wave intensities show clear peaks around 1.44 GeV/c^2 that result from the production and decay of the tensor $K_2^*(1430)$. The intensity distributions for the $2^+0^-K^*D$ and the $2^+0^-\rho D$ partial waves are shown in fig. 3(b) The evidence for resonant behavior in the $2^+0^-\rho D$ amplitude is somewhat equivocal; not only does the $2^+0^-\rho D$ intensity have more apparent background above the peak but its phase also moves backward relative to the phase of the $2^+0^-K^*D$ wave indicating that it may have a sizable nonresonant background contribution. These waves also show an enhancement around 2 GeV/c^2; this effect will be quantitatively discussed in a following subsection.

It is possible to fit the intensities and relative phases of these 2^+ waves to a D wave Breit-Wigner and a background amplitude, but the quality of the fit depends on the form of the background for the $2^+0^-\rho D$. To extract the $K_2^*(1430)$ resonance parameters in a relatively model-independent way, a fit to

the $2^+0^-K^*D$, $2^+1^+K^*D$, and $2^+0^-\rho D$ differential cross sections was performed ignoring the relative phases of the two coherent $\eta-$ waves. The results of this fit are listed in table 2 and the predicted lineshapes for the $2^+0^-K^*D$ and $2^+0^-\rho D$ waves are shown in fig. 3(b). The quoted peak value for the $K^*\pi$ differential cross section is the sum of the $M = 0$ and $M = 1$ contributions. The value for the $K\rho/K^*\pi$ branching ratio is in good agreement with the averaged world data [21].

Table 2

The 2^+ $K_2^*(1430)$ parameters. The differential cross sections are quoted at the peak of the resonance in events/(0.02 GeV/c^2). The $K^*\pi$ differential cross section is the sum of the $M = 0$ and $M = 1$ contributions, and the $K\rho/K^*\pi$ branching ratio is corrected for isospin.

$K_2^*(1430) \rightarrow 2^+0^-K^*D$ / $2^+0^-\rho D$	
Mass (GeV/c^2)	$1.434 \pm 0.004 \pm 0.006$
Width (GeV/c^2)	$0.129 \pm 0.015 \pm 0.015$
χ^2/DOF	27.0/18
$d\sigma/dM_3(K^*\pi)$	$970 \pm 71 \pm 60$
$d\sigma/dM_3(K\rho)$	$213 \pm 29 \pm 15$
$BR(K\rho/K^*\pi)$	$0.293 \pm 0.032 \pm 0.020$

3.3 The 3^- $K_3^*(1780)$

The bumps in the two 3^- partial wave cross sections around 1.75 GeV/c^2 are the expected signature of the F wave $K_3^*(1780)$. In fitting these distributions, which are displayed in fig. 3(c), a background contribution is hardly justified

as they both show a resonance-like structure with little background at higher $\bar{K}^0\pi^+\pi^-$ masses. In addition, the $3^-0^-K^*F$ and $3^-0^-\rho F$ amplitudes are approximately in phase up to a mass of ~ 2 GeV/c^2. Hence, the 3^- intensities and relative phases are fit to a common Breit-Wigner lineshape without a background amplitude, the relative phase offset of the two amplitudes being a fit parameter.

The results of the fit are listed in table 3. Because the 3^- cross sections do not require a nonresonant component in their parametrizations, the systematic uncertainties of the differential cross sections are substantially reduced compared to the systematic uncertainties for the 2^+ $K_2^*(1430)$. On the other hand, the statistical errors are larger because of the smaller resonance signal. The lineshapes predicted by the fit, shown in fig. 3(c), are in good agreement with the measured cross sections. The $K\rho/K^*\pi$ branching ratio is in mild disagreement with the 95% confidence level (CL) upper limit of 0.77 quoted in ref. [14], but is in agreement with most quark model predictions of approximately equal partial widths for the $K\rho$ and $K^*\pi$ decay modes. The fitted angle is the phase of the combined production and decay amplitude for the $K_3^*(1780) \rightarrow K\rho$ wave relative to the same combination for the $K^*\pi$ decay.

The 3^- $K_2^*\pi$ partial waves are not statistically significant and so were not included in the set of fitted partial waves. Therefore, to place an upper limit for the $K_3^*(1780)$ partial width into $K_2^*\pi$, the partial wave fits were repeated with the inclusion of the $3^-0^-K_2^*D$ wave. The measured $3^-0^-K_2^*D$ intensity in the region of the $K_3^*(1780)$ is then used to estimate the amount of 3^- $K_2^*\pi$ cross section that could be associated with the $K_3^*(1780)$. This value is quoted in table 3, but since the $3^-0^-K_2^*D$ wave shows no significant structure this estimate should properly be used to place an upper limit on the $K_3^*(1780)$ partial width into the

Table 3

The 3^- $K_3^*(1780)$ parameters. The differential cross sections are quoted at the peak of the resonance in events/(0.02 GeV/c^2). The branching ratios are corrected for isospin, and for the $K^*(1430) \to K\pi$ branching fraction.

$K_3^*(1780) \to 3^-0^-K^*F$ / $3^-0^-\rho F$ / $3^-0^-K_2^*D$	
Mass (GeV/c^2)	$1.740 \pm 0.014 \pm 0.015$
Width (GeV/c^2)	$0.171 \pm 0.042 \pm 0.020$
χ^2/DOF	16.6/17
$d\sigma/dM_3(K^*\pi)$	$201 \pm 36 \pm 14$
$d\sigma/dM_3(K\rho)$	$229 \pm 53 \pm 15$
$d\sigma/dM_3(K_2^*\pi)$	36 ± 17
$BR(K\rho/K^*\pi)$	$1.52 \pm 0.21 \pm 0.10$
$BR(K_2^*\pi/K^*\pi)$	< 0.78 (95% CL)
$\phi(K\rho$ wrt $K^*\pi)$ (rad)	$3.26 \pm 0.10 \pm 0.05$

$K_2^*\pi$ final state. Such an upper limit is quoted in table 3 for the $K_2^*\pi$ to $K^*\pi$ branching ratio; in addition to the isospin correction, this branching ratio has also been corrected for the $K_2^*(1430)$ branching fraction into $K\pi$ [21].

3.4 The 1^- Resonant States

The behavior of the $1^-0^-K^*P$ and $1^-0^-\rho P$ cross sections and relative phases, shown in fig. 4, indicates that these amplitudes have at least two resonant parts, one at low mass contributing only to the $1^-0^-K^*P$ wave and the other at high mass contributing to both the $1^-0^-K^*P$ and $1^-0^-\rho P$ cross sections. A model with these ingredients provides a good description of the data.

The 2^+ wave, being dominated by the $K_2^*(1430)$, is used to define the absolute phase behavior in the mass region below 1.6 GeV/c^2, while above this mass the absolute phase behavior is determined by the 3^- partial waves. The $1^-0^-K^*P$

amplitude is assumed to be dominated by a resonance in the region of 1.4 GeV/c^2, and at higher mass by the same resonance that describes the behavior of the $1^-0^-\rho P$ amplitude. A quadratic background is allowed to contribute coherently to the $1^-0^-K^*P$ amplitude, but this term is not necessary to achieve a reasonable fit.

The complete fit, which has 18 free parameters describing the 1^- amplitudes and the relative phases of the $2^+0^-K^*D$ and the 3^- waves, is used to estimate the masses, widths, and normalizations of the two 1^- resonances. The 2^+ $K_2^*(1430)$ and 3^- $K_3^*(1780)$ resonance parameters are fixed to those listed in table 2 and table 3, respectively. The results of the fit are listed in table 4.

The predicted and observed intensities and phases for the $2^+0^-K^*D$ and the 3^- waves are shown in fig. 5 and the similar comparison for the two 1^- waves is shown in fig. 4. This five-wave model is able to reproduce all of the features of the measured amplitudes quite well. The $1^-0^-K^*P$ amplitude is understood to arise from the coherent sum of the two P wave resonances. The fit determines that the product of the production and decay coupling phase for the higher mass resonance is $\sim 220°$ forward of the same phase for the lower mass resonance. This implies that the leading edge of the broad, higher mass state interferes destructively with the lower mass resonance as the phase of the lower mass state advances through 90°. At higher mass, this interference continues to be destructive as the absolute phase of the lower mass state approaches 180° while the higher mass state resonates.

Table 4

The results of the 1^- fits. The parameters of the 1^- states determined by the three different fits are listed below. The low and high mass states are denoted as K_a^* and K_b^*, respectively.

Fit to the $2^+0^-K^*D$, the 1^-, and the 3^- waves.	
Mass_a (GeV/c^2)	$1.420 \pm 0.007 \pm 0.010$
Width_a (GeV/c^2)	$0.240 \pm 0.018 \pm 0.012$
Mass_b (GeV/c^2)	$1.735 \pm 0.010 \pm 0.020$
Width_b (GeV/c^2)	$0.423 \pm 0.018 \pm 0.030$
χ^2/DOF	125/73
$d\sigma/dM_3(K_a^* \to K^*\pi)$	$1991 \pm 133 \pm 150$
$d\sigma/dM_3(K_b^* \to K^*\pi)$	$1146 \pm 76 \pm 170$
$d\sigma/dM_3(K_b^* \to K\rho)$	$813 \pm 42 \pm 30$
$BR(K_b^* \to K\rho/K_b^* \to K^*\pi)$	$0.97 \pm 0.09^{+0.30}_{-0.10}$
$\phi(K_3^*(1780) \to K^*\pi$ wrt $K_a^* \to K^*\pi)$ (rad)	$2.63 \pm 0.06 \pm 0.05$
$\phi(K_3^*(1780) \to K\rho$ wrt $K_a^* \to K^*\pi)$ (rad)	$5.77 \pm 0.12 \pm 0.05$
$\phi(K_2^*(1430) \to K^*\pi$ wrt $K_a^* \to K^*\pi)$ (rad)	$5.05 \pm 0.09 \pm 0.05$
$\phi(K_b^* \to K^*\pi$ wrt $K_a^* \to K^*\pi)$ (rad)	$3.99 \pm 0.03 \pm 0.05$
$\phi(K_b^* \to K\rho$ wrt $K_a^* \to K^*\pi)$ (rad)	$0.36 \pm 0.05 \pm 0.05$

3.5 THE 4^+ AMPLITUDES

The summed 4^+ cross section shows a bump at ~2.1 GeV/c^2, but the significance of this structure in the individual 4^+ partial waves is difficult to estimate (cf. fig. 6). The observed enhancement is consistent with the production and decay of the G wave $K_4^*(2060)$ but it is not possible to ascribe it unambiguously to this state because the measured relative phases are too unreliable to determine if the amplitudes behave resonantly.

However, if one assumes that the bulk of the enhancement is due to $K_4^*(2060)$ production and decay, it is then possible to estimate its branching fractions into the $K^*\pi$, $K\rho$, and $K_2^*\pi$ decay modes. In fig. 6, the $4^+0^-K^*G$ intensity shows the clearest indication of a bump and so there is little systematic uncertainty involved in estimating its size; the $4^+0^-\rho G$ and the $4^+0^-K_2^*F$ partial waves, on the other hand, do not show an obvious resonant signal, which makes it difficult to determine the size of the resonant component. For this reason, upper limits are also quoted for the $K_4^*(2060)$ differential cross sections into these final states. The 4^+ partial wave intensities are fit to a common resonant lineshape assuming no background contribution to the amplitudes. The mass and width of the resonance are fixed at 2.060 and 0.200 GeV/c^2, respectively, these values being reasonable choices based on the two published measurements of this state [2,3], and the resulting fitted line-shapes are shown as the curves in fig. 6. By assuming no background terms in the fit, conservative upper limits for the 4^+ $K\rho$ and $K_2^*\pi$ differential cross sections can be obtained from the fitted peak intensities and their uncertainties. (Allowing a background does not alter the fit result for the $4^+0^-K^*G$ peak intensity, but does reduce the size of the resonant contribution to the $4^+0^-\rho G$ and $4^+0^-K_2^*F$ intensities.) These fitted peak intensities and their corresponding 95% CL upper limits are given in table 5.

3.6 The 2^+ Amplitudes at High Mass

The $2^+0^-K^*D$ and the $2^+0^-\rho D$ intensities show a large enhancement at ~2.0 GeV/c^2, which may be evidence for a second resonant 2^+ state. To test this hypothesis, the intensities and relative phases of these two waves are fit to a resonant lineshape in the mass region above 1.69 GeV/c^2. The absolute phase

Table 5

The results of the 4^+ fits. The values are obtained assuming that all of the 4^+ intensity results from $K_4^*(2060)$ production, and are expressed in units of events/(0.02 GeV/c^2). These values have not been corrected for isospin or for the branching fraction of the $K_2^*(1430)$ into $K\pi$.

Final State	$d\sigma/dM_3$ at Peak	
	Fitted Value	95% CL Upper Limit
$K^*\pi$	$120 \pm 26 \pm 17$	≤ 173
$K\rho$	$50 \pm 14 \pm 15$	≤ 137
$K_2^*\pi$	$42 \pm 14 \pm 15$	≤ 82

is set by using the phase behavior of the $1^-0^-K^*P$ reference wave determined from the simultaneous fit to the $1^-0^-K^*P$, the $1^-0^-\rho P$, the $2^+0^-K^*D$, and the 3^- waves.

It is not possible to achieve a good fit to a model with a single resonance without including a background term which is significant above 2 GeV/c^2. Therefore a coherent, linearly-rising background is introduced into the amplitude parametrization for both 2^+ waves. The fitted resonance parameters are insensitive to the detailed form of this background. The results of the fit are shown in table 6.

The predicted lineshapes are compared with the measured intensities and phases in fig. 7. The agreement with the data is reasonable, although the measured intensities behave somewhat erratically. The measured absolute phases, which show ~90° of forward motion, are well reproduced by the fit. These results confirm that a resonance interpretation of the 2^+ enhancement is consistent with the data.

However, a stronger conclusion without additional data is not warranted. First, although the intensities of the $2^+0^-K^*D$ and the $2^+0^-\rho D$ rise abruptly

Table 6

The fits to the high mass 2^+ amplitudes. The differential cross sections are quoted at the peak of the resonance in events/(0.02 GeV/c^2). The $K\rho/K^*\pi$ branching ratio is corrected for isospin.

Fit to the High Mass $2^+0^-K^*D$ and $2^+0^-\rho D$ Amplitudes	
Mass (GeV/c^2)	$1.973 \pm 0.008 \pm 0.025$
Width (GeV/c^2)	$0.373 \pm 0.033 \pm 0.060$
χ^2/DOF	32.1/21
$d\sigma/dM_3(K^*\pi)$	$230 \pm 34 \pm 14$
$d\sigma/dM_3(K\rho)$	$448 \pm 36 \pm 15$
$BR(K\rho/K^*\pi)$	$1.49 \pm 0.24 \pm 0.09$
$\phi(K\rho$ wrt $K^*\pi)$ (rad)	$0.45 \pm 0.10 \pm 0.05$

around 1.8–1.9 GeV/c^2, their persistence above 2.1 GeV/c^2 raises questions about the uniqueness of the single resonance interpretation. In fact, the data cannot exclude a two-resonance model with the second resonance being somewhat higher in mass. Secondly, the interpretation of the phase information is model-dependent because the absolute phase is set using the two-resonance model of the 1^- waves; this is perhaps not a serious problem as the behavior of the 3^- waves constrains the absolute phase of the reference wave up to a mass of $\sim$ 1.9 GeV/c^2. Thirdly, the behavior of the $2^+0^-K_2^*P$ amplitude does not appear to be completely consistent with this interpretation; its intensity does not show a comparable enhancement around 2 GeV/c^2 in mass but its relative phase behavior mimics that of the other 2^+ waves. It is possible that the $2^+0^-K_2^*P$ has a resonant component but the lack of structure in its intensity makes such an interpretation uncertain.

4. Discussion

4.1 The Well-Established States

The PWA has identified several states, some of which are well-established $q\bar{q}$ excitations. The tensor $K_2^*(1430)$ is the 1^3P_2 member of the $L = 1$ orbital excitation. The axial-vector $K_1(1400)$ is understood to be almost equal mixtures of the two lowest-lying 1^+ strange mesons, the 1^1P_1 and the 1^3P_1; since the strange mesons are not charge-conjugation eigenstates, such singlet–triplet mixing is allowed. The unseen member of the $L = 1$ multiplet, the 0^+ $K_0^*(1350)$, cannot decay to $\bar{K}^0\pi^+\pi^-$ because of parity conservation.

The next leading natural spin-parity state, the 3^- $K_3^*(1780)$, is the obvious candidate for the 3^- resonance structure in the $K^*\pi$ and $K\rho$ final states. Although the observed mass of this resonance is about 0.04 GeV/c^2 below the world average of ~1.780 GeV/c^2, the disagreement is less than a two standard deviation effect. This state is a member of the $L = 2$ multiplet, namely the 1^3D_3.

The PWA shows evidence for the production and decay of the 4^+ $K_4^*(2060)$, although resonant behavior is not clearly required by the data. This resonance is the leading member of the $L = 3$ multiplet, the 1^3F_4, and has been observed previously only in the $K\pi$ decay mode.

4.2 The Interpretation of the 1^- States

The behavior of the two 1^- partial waves is well understood in terms of a model that incorporates a resonant state with a mass and width of 1.42 and 0.23 GeV/c^2, respectively, coupling only to the $K^*\pi$ decay mode, and a second state with a mass and width of 1.73 and 0.43 GeV/c^2, respectively, that couples

to both the $K\rho$ and $K^*\pi$ final states. This confirms the essential results of the most recent $\bar{K}^\circ \pi^+\pi^-$ PWA [14] where these two states were observed and called the $K^*(1410)$ and the $K^*(1790)$. The higher mass state is now measured to be significantly lower in mass and broader than in ref. [14], but the observed behavior of the amplitudes in the two analyses is consistent. It appears that the disagreement in mass and width results from the explicit parametrization of the data. If the measured 1^- waves are fit using the parametrization employed in ref. [14], the fitted mass increases by $\sim$0.05 GeV/c^2 and the width decreases by $\sim$0.05 GeV/c^2. This difference in parametrization arises from the failure of the authors in ref. [14] to include the effect of three-body phase space on the resonance lineshape; the increasing phase space as a function of three-body mass implies that the observed resonance peak in the differential cross section will be shifted up in mass by an amount that depends on the width of the structure. For a resonance with a width of 0.4 GeV/c^2, this mass shift turns out to be $\sim$0.04 GeV/c^2.

In the quark model, these two vector states may be:

1. the 2^3S_1 state, which is the first radial excitation of the $K^*(892)$;
2. the 1^3D_1 level, which is the member of the $L = 2$ multiplet containing the 3^- $K_3^*(1780)$; and
3. the 3^3S_1, which is the second radial excitation of the $K^*(892)$.

The other candidate $q\bar{q}$ 1^- states are heavier radial excitations of these three and can be ruled out because their expected masses are too high. It is conceivable that the observed resonances could be mixtures of these three candidate

states[♯2] and this possibility cannot be excluded *a priori*. However, it is argued below that the lower mass state is predominantly 2^3S_1 while the upper state must be mostly 1^3D_1.

The proximity in mass of the $K^*(1790)$ and the 3^- $K_3^*(1780)$ makes the association of the high mass state with the 1^3D_1 quite attractive. Besides this small splitting, the total and partial widths of the high mass 1^- state agree fairly well with those predicted by various quark model calculations. In contrast, the mass of the $K^*(1410)$ is so far below the mass of the 3^- $K_3^*(1780)$ that its assignment as the triplet partner to the 3^- can be safely ruled out. This means that the $K^*(1410)$ can be simply understood only as the radial excitation of the $K^*(892)$; this then raises the possibility that the 1^- $K^*(1790)$ is the second radial excitation of the $K^*(892)$, or some mixture of this state and the 1^3D_1 state.

Most theoretical predictions for the mass of the radial excitation of the $K^*(892)$ place it around 1.5–1.7 GeV/c^2, in disagreement with the assignment of the $K^*(1410)$. However, the observed decay properties of this resonance tend to support its interpretation as a radial excitation. Several quark model calculations [22–24] have indicated that the decay of a radial excitation of a $^3S_1$ state into a two-body final state with a large center-of-mass (CMS) kinetic energy is suppressed relative to decay modes with smaller values of CMS momentum; this suppression arises from the radial node(s) in the wave function of a radially excited state. Although these calculations are model-dependent because of the way relativistic effects are incorporated, the prediction of a weak two-body

♯2 Such mixing of pure $q\overline{q}$ states to yield the physically observed states is not without precedent in meson spectroscopy: in the strange meson sector, the two 1^+ states $K_1(1280)$ and $K_1(1400)$ (as mentioned above) are believed to be mixtures of the 1^1P_1 and the 1^3P_1 quark model states; and in the charmonium sector, the 2^3S_1 and the 1^3D_1 states mix weakly to give the observed $\psi(3685)$ and the $\psi(3770)$.

coupling for the radially excited vector states is a persistent result. This prediction has the following consequences: in the strange sector, the radial excitations should prefer to couple to $K^*\pi$ or $K\rho$ and not to $K\pi$; the radially excited isovectors should not couple strongly to the $\pi\pi$ decay mode; and the charmonium radial excitations should decay strongly into states such as $D^*\bar{D}$ and $D^*\bar{D}^*$ and not into $D\bar{D}$.

There are a number of experimental observations that support this predicted decay systematic. In the charmonium sector, the $\psi(4030)$ (the 3^3S_1 $c\bar{c}$ state) prefers to decay via $D^*\bar{D}^*$ instead of $D\bar{D}$ although the former is very close to threshold. The situation with the isovectors is still quite confused, but a consistent interpretation of the data is possible that not only agrees with the model predictions but also explains several mysteries. The two candidates for the first radial excitation of the $\rho(770)$ are the $\rho(1250)$ and the $\rho(1600)$. The $\rho(1250)$ has only been seen in the $\omega\pi$ decay mode with little evidence of it in $\pi\pi$ final states. If we assume that it is a real 1^- state, then it can be understood only as the first radial excitation of the $\rho(770)$ on the basis of the arguments used above in the case of the $K^*(1410)$. Its lack of coupling to $\pi\pi$ would then be a reflection of its radial nature. This interpretation of the $\rho(1250)$ fits in nicely with the assignment for the $K^*(1410)$, as the mass splitting of the two states agrees with that expected for the strange and isovector states of the same nonet. This also implies that the $\rho(1600)$ is probably the 1^3D_1 partner of the $\rho_3(1690)$. However, it should be noted that the status of the $\rho(1250)$ is very poor; the most recent photoproduction experiment analyzing the $\omega\pi$ channel could not unambiguously confirm or deny its existence [25], while a recent analysis of the same channel produced in e^+e^- collisions appears to rule it out [26].

In summary, the interpretation of the $K^*(1410)$ as the 2^3S_1 state is preferred. Its assignment as the 1^3D_1 is not tenable, as this implies large $L = 2$ multiplet mass splittings. The higher mass 1^- state could conceivably correspond to a superposition of the 1^3D_1 and the 3^3S_1 states; however, in light of the arguments presented for the $K^*(1410)$, the observation of a strong $K\pi$ decay mode [3] would suggest that its interpretation as 1^3D_1 is the more likely.

4.3 The Higher Mass 2^+ State

The second resonance-like enhancement in the 2^+ amplitudes at $\sim$1.97 GeV/c^2 has two possible quark model interpretations: (a) it is the 2^3P_2, *i.e.* the radial recurrence of the $K_2^*(1430)$; or, (b) it is the 1^3F_2, the partner to the 4^+ $K_4^*(2060)$. Two comments can be made concerning the possible assignment:

1. The mass of the 2^3P_2 state predicted by Godfrey and Isgur [27] is $\sim$1.94 GeV/c^2, which is in good agreement with the estimated mass of the resonance. In contrast, the 1^3F_2 state is expected to be nearly degenerate with the $K_4^*(2060)$ as the multiplet splittings are expected to (and do!) decrease with increasing orbital excitation. However, because the theoretical uncertainty of these mass splittings is quite large, the orbital assignment cannot be ruled out.

2. A candidate for the 2^3P_0 state has been observed in the $K\pi$ data [3] at a mass of $\sim$1.9 GeV/c^2. The association of the 2^+ state with this resonance is implied from the small mass splittings between these two states.

Although each of the above arguments favors the radial interpretation, both are weak and so a definite assignment is not possible; it is conceivable that both of

the expected 2^+ states are being observed, which may account for the "flat-top" appearance of the 2^+ partial wave intensities above 2.0 GeV/c^2.

5. Conclusions

The behavior of the $\bar{K}^\circ \pi^+\pi^-$ partial wave amplitudes is well described by a model incorporating several resonance contributions. This model is able to reproduce the observed structures in the differential cross sections, as well as the measured relative phase behavior of the coherent partial waves. The masses, widths, and branching fractions of several strange meson states are obtained by fitting this model to the extracted partial wave amplitudes. The most likely quark model state assignments and our results are summarized in table 7 and fig. 8; the latter also includes a comparison of the measured and predicted [27] mass values.

The $1^+0^+K^*S$ amplitude shows a clear $K_1(1400)$ structure sitting on little background. The fit to this amplitude provides a new measure of the mass and width of the $K_1(1400)$ without the complications introduced by the large non-resonant 1^+ amplitudes present in the diffractively produced $K\pi\pi$ final state. The 2^+ $K_2^*(1430)$, a triplet partner to the $K_1(1400)$, accounts for the large enhancement in the $2^+0^-K^*D$ and $2^+0^-\rho D$ cross section around 1.44 GeV/c^2. Its measured mass, width, and ratio of partial widths into $K\rho$ and $K^*\pi$ confirm the previously measured properties of this state.

A second enhancement in the 2^+ cross section, observed at $\sim$2 GeV/c^2 decaying into both $K\rho$ and $K^*\pi$, is consistent with a resonance interpretation. The fit to both decay modes assuming a single resonance gives a mass and width of 1.97 and 0.37 GeV/c^2, respectively. Two strange $q\bar{q}$ excitations are expected in this

Table 7

The most likely quark model assignments and measured mass values for the resonant $\bar{K}^\circ \pi^+\pi^-$ states observed in this experiment (all seen in $K^*\pi$); other seen decay modes and relative branching ratios are also given. Quoted errors are obtained as the sum of the statistical and systematic errors.

Spin-Parity (isobar)	Probable $q\bar{q}$ state	Measured Mass (GeV/c^2)	Other Decays	Branching Ratio ($K^*\pi \equiv 1$)
$1^- K^*\pi$	$2\,^3S_1$	1.420 ± 0.017		
	$1\,^3D_1$	1.735 ± 0.030	ρK	$0.97^{+0.39}_{-0.19}$
$2^+ K^*\pi$	$1\,^3P_2$	1.434 ± 0.010	ρK	0.29 ± 0.05
	$2\,^3P_2$	1.973 ± 0.033	ρK	1.49 ± 0.33
$3^- K^*\pi$	$1\,^3D_3$	1.740 ± 0.029	ρK	1.52 ± 0.31
			$K_2^*\pi$	< 0.78
4^+	$1\,^3F_4$	2.060 [2,3]	$K^*\pi$	probably seen
$1^+ K^*\pi$	$1\,^{1,3}P_1$	1.373 ± 0.032		

mass region: the first radial recurrence of the 1^3P_2 $K_2^*(1430)$ and the partner to the 1^3G_4 $K_4^*(2060)$.

The mass and width of the 3^- $K_3^*(1780)$ state are measured using both the $K^*\pi$ and the $K\rho$ final states, the ratio of partial widths of these two modes being ~ 1. No evidence for a $K_2^*\pi$ decay mode is found, but an upper limit is obtained for the $K_2^*\pi$ branching fraction.

The 1^- partial waves are shown to arise from the production and decay of two states. The lower in mass is almost degenerate with the $K_2^*(1430)$, having a mass and width of $1.420 \pm 0.007 \pm 0.010$ and $0.240 \pm 0.018 \pm 0.012$ GeV/c^2, respectively, and decaying only to $K^*\pi$. The second state has a mass and width of $1.735 \pm 0.010 \pm 0.020$ and $0.423 \pm 0.018 \pm 0.030$, respectively, and decays to

$K\pi$, $K^*\pi$, and $K\rho$. The properties of the lower mass state are consistent with its assignment as the first radial excitation of the 1^- $K^*(892)$. These data confirm the results of a prior analysis of the $\bar{K}^\circ \pi^+\pi^- n$ final state [14] where the two states were observed and called the $K^*(1410)$ and the $K^*(1790)$.

A small 4^+ signal is seen that is consistent with the mass and width of the $K_4^*(2060)$; however, it is possible only to set upper limits on the production cross section times branching fraction for the $K_4^*(2060)$ decay modes to $\bar{K}^\circ \pi^+\pi^-$.

REFERENCES

[1] P. Estabrooks et al., Nucl. Phys. B133 (1978) 490.

[2] W.E. Cleland et al., Nucl. Phys. B208 (1982) 189.

[3] D. Aston et al., Phys. Lett. 106B (1981) 235.

[4] Yu. Antipov et al., Nucl. Phys. B86 (1975) 365.

[5] G. Otter et al., Nucl. Phys. B93 (1975) 365.

[6] T. Tovey et al., Nucl. Phys. B95 (1975) 109.

[7] G.W. Brandenburg et al., Phys. Rev. Lett. 36 (1976) 703.

[8] J.S.M. Vergeest et al., Phys. Lett. 62B (1976) 471.

[9] R.K. Carnegie et al., Nucl. Phys. B127 (1977) 509.

[10] E. Konigs et al., Phys. Lett. 74B (1978) 282.

[11] A. Etkin et al., Phys. Rev. D22 (1980) 42.

[12] C. Daum et al., Nucl. Phys. B187 (1981) 1.

[13] M. Baubillier et al., Nucl. Phys. B202 (1982) 21.

[14] D. Aston et al., Nucl. Phys. B247 (1983) 261.

[15] P.K. Sinervo, SLAC-REP-299, May 1986 (Ph.D. Thesis).

[16] J. D. Jackson, Nuovo Cimento 34 (1964) 1144.

[17] W. Dunwoodie et al., Group B Physics Note # 60 (unpublished).

[18] J.M. Blatt and V.F. Weisskopf, Theoretical Nuclear Physics, (Wiley, New York, 1952), 361.

[19] F. James and M. Roos, CERN Program Library, D506.

[20] T.G. Trippe et al., Rev. Mod. Phys. 48 (1976) S1.

[21] Particle Data Group, Phys. Lett. 170B (1986).

[22] A. Bradley, J. Phys. G4 (1978) 1517.

[23] E. Eichten et al., Phys. Rev. D21 (1980) 203.

[24] S.B. Gerasimov et al., Z. Phys. C13 (1982) 43.

[25] M. Atkinson et al., Nucl. Phys. B243 (1984) 269.

[26] S. I. Dolinsky et al., Phys. Lett. 174B (1986) 453.

[27] S. Godfrey and N. Isgur, Phys. Rev. D32 (1985) 189.

FIGURE CAPTIONS

Fig. 1. The $\bar{K}^\circ \pi^+\pi^-$ invariant mass distribution. The outer histogram is for the entire data sample, whereas the inner histogram is for events with $|t'| \leq 0.3$ (GeV/c)^2. The dashed line shows the acceptance for the final event selection as a function of $m(\bar{K}^\circ \pi^+\pi^-)$.

Fig. 2. The spin-parity wave sums. The intensities of the summed partial waves with the same J^P are plotted as a function of mass. The intensities include the interference terms between coherent waves.

Fig. 3. The fits to the 1^+, 2^+, and 3^- intensities. The fit of the $K_1(1400)$ resonance to the $1^+0^+K^*S$ cross section is shown in (a), the fit of the $K_2^*(1430)$ resonance to the $2^+0^-K^*D$ and $2^+0^-\rho D$ cross sections is presented in (b), and the fit of the $K_3^*(1780)$ resonance to the $3^-0^-K^*F$ and $3^-0^-\rho F$ intensities is shown in (c).

Fig. 4. The five-wave fit predictions for the 1^- waves. The phases are set using the predicted behavior of the $1^-0^-K^*P$ reference wave.

Fig. 5. The five-wave fit predictions for the 2^+ and 3^- waves. The phases are set using the predicted behavior of the $1^-0^-K^*P$ reference wave.

Fig. 6. The fits to the 4^+ intensities. The curves correspond to a Breit-Wigner line-shape for mass 2.06 GeV/c^2 and width 0.20 GeV/c^2.

Fig. 7. The fitted 2^+ lineshapes at high mass. The relative phases are set using the predicted behavior of the $1^-0^- K^*P$ reference wave above a mass of 1.69 GeV/c^2; below this mass, the phase of the reference wave is not set.

Fig. 8. The most likely quark model state assignments and measured mass values for the resonant $\bar{K}^\circ\pi^+\pi^-$ amplitudes obtained in this experiment; the shaded regions correspond to the errors quoted in table 7; the mass predictions from ref. 27 are also shown.

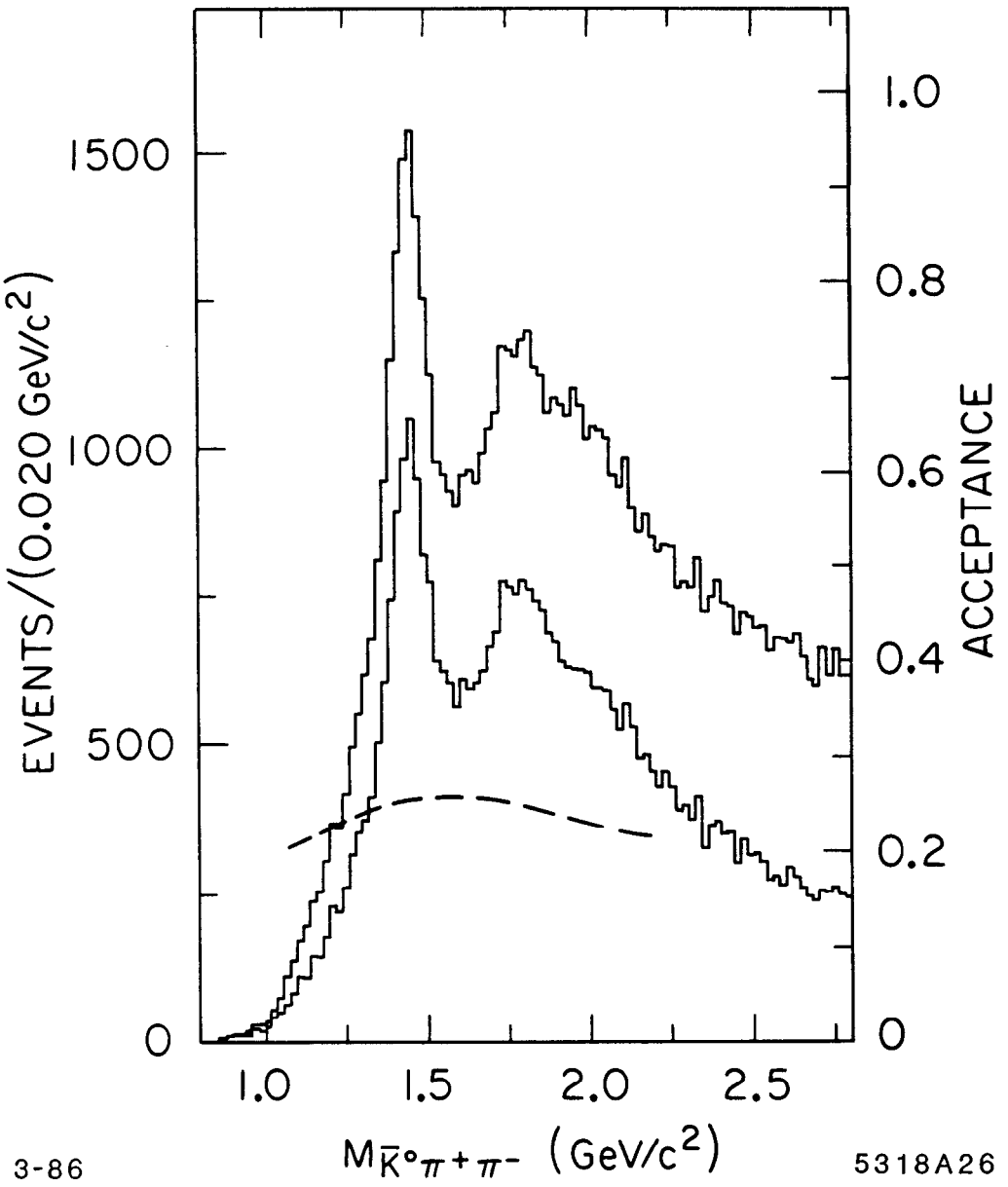
1500
1000
500
0
EVENTS/(0.020 GeV/c²)
1.0
0.8
0.6
0.4
0.2
0
ACCEPTANCE
1.0
1.5
2.0
2.5
M K̄°π+π- (GeV/c²)
3-86
5318A26

Fig. 1

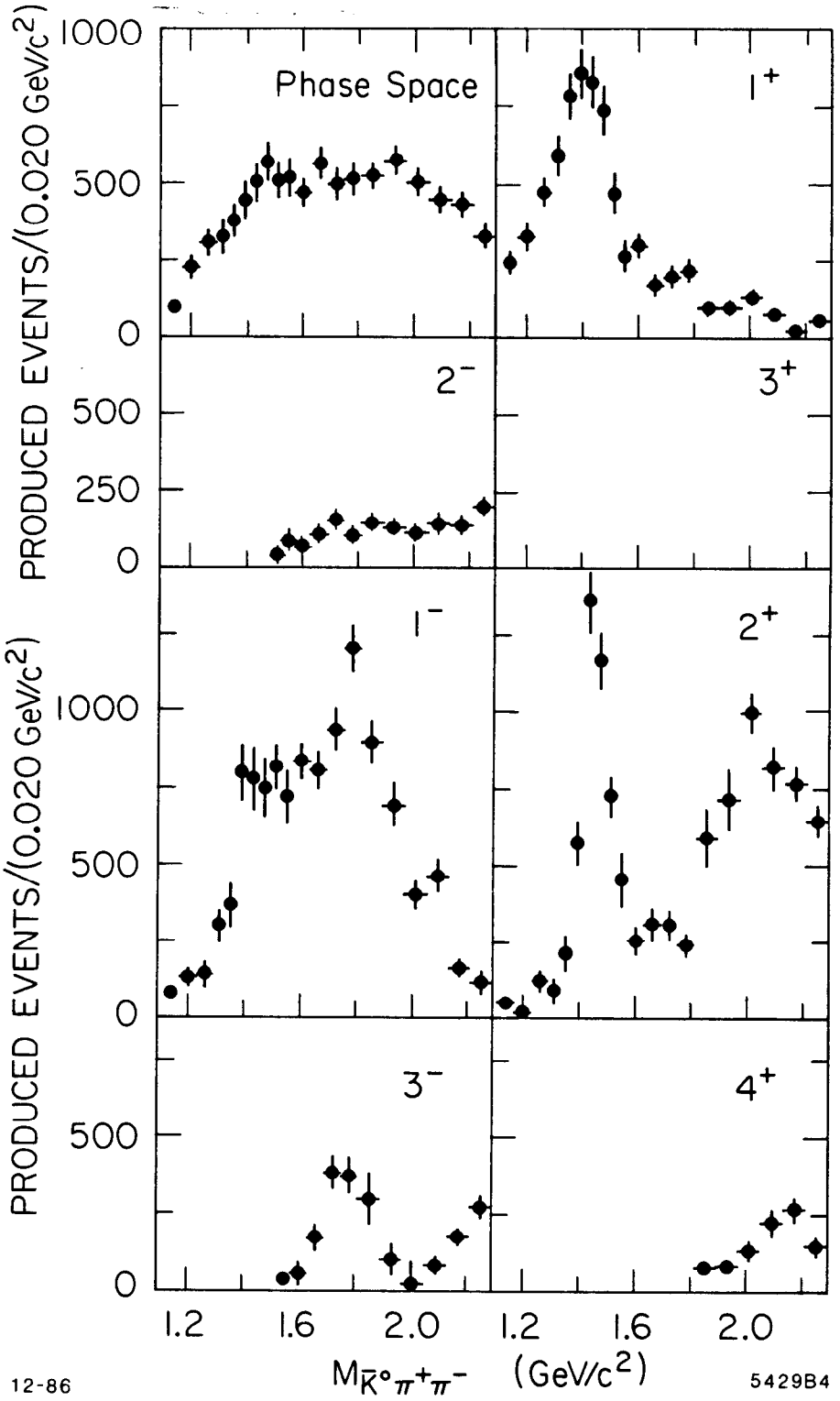
Phase Space
1+
2−
3+
1−
2+
3−
4+
PRODUCED EVENTS/(0.020 GeV/c²)
1000
500
0
250
1.2
1.6
2.0
M K̄°π+π− (GeV/c²)
12-86
5429B4

Fig. 2

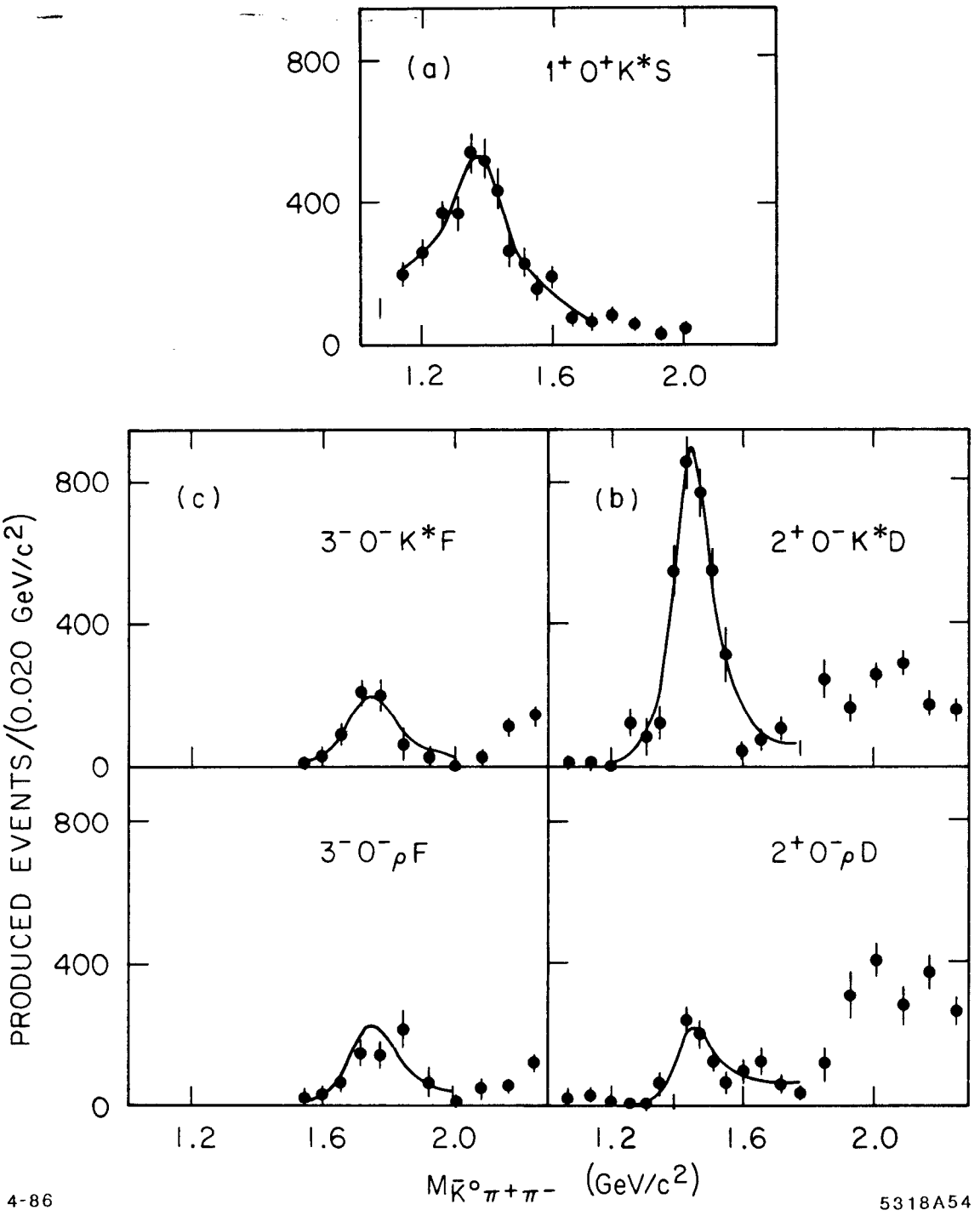
(a)
1+ 0+ K*S
(c)
3- 0- K*F
(b)
2+ 0- K*D
3- 0- ρF
2+ 0- ρD
800
400
0
1.2
1.6
2.0
PRODUCED EVENTS/(0.020 GeV/c2)
M K̄0π+π- (GeV/c2)
4-86
5318A54

Fig. 3

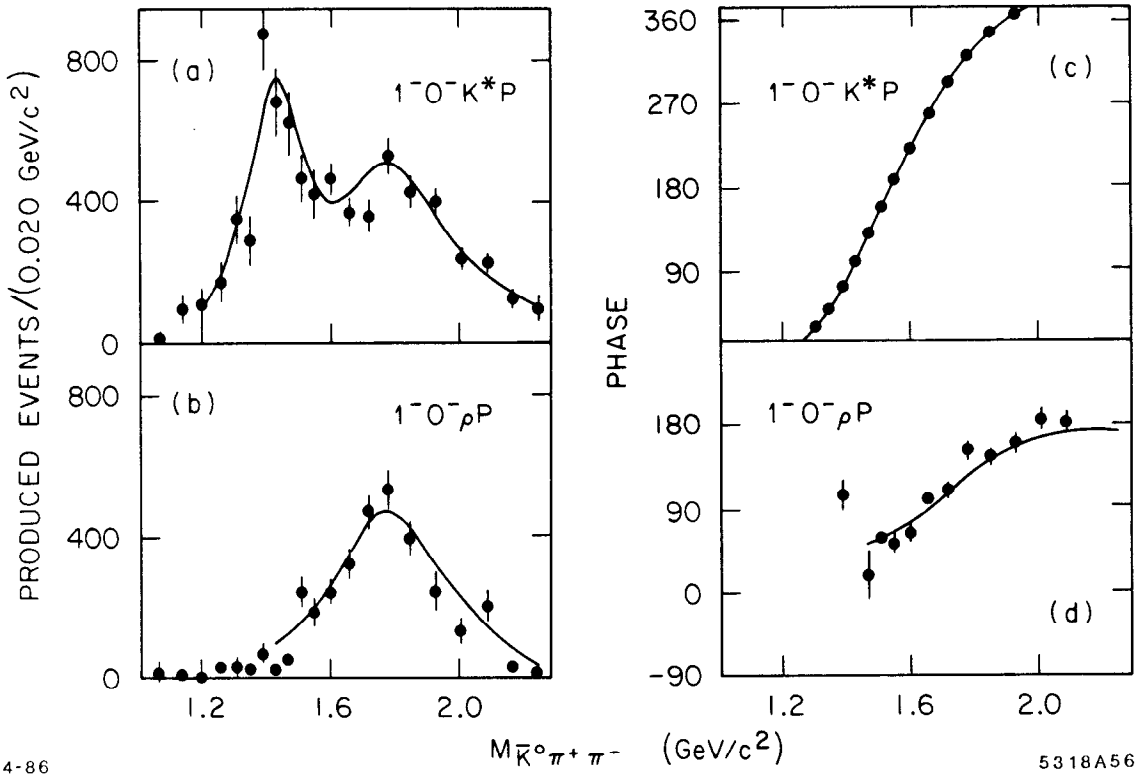
PRODUCED EVENTS/(0.020 GeV/c²)
800
400
0
(a)
1⁻0⁻K*P
800
400
0
(b)
1⁻0⁻ρP
1.2
1.6
2.0
Mκ°π⁺π⁻ (GeV/c²)
PHASE
360
270
180
90
(c)
1⁻0⁻K*P
180
90
0
-90
(d)
1⁻0⁻ρP
1.2
1.6
2.0
4-86
5318A56

Fig. 4

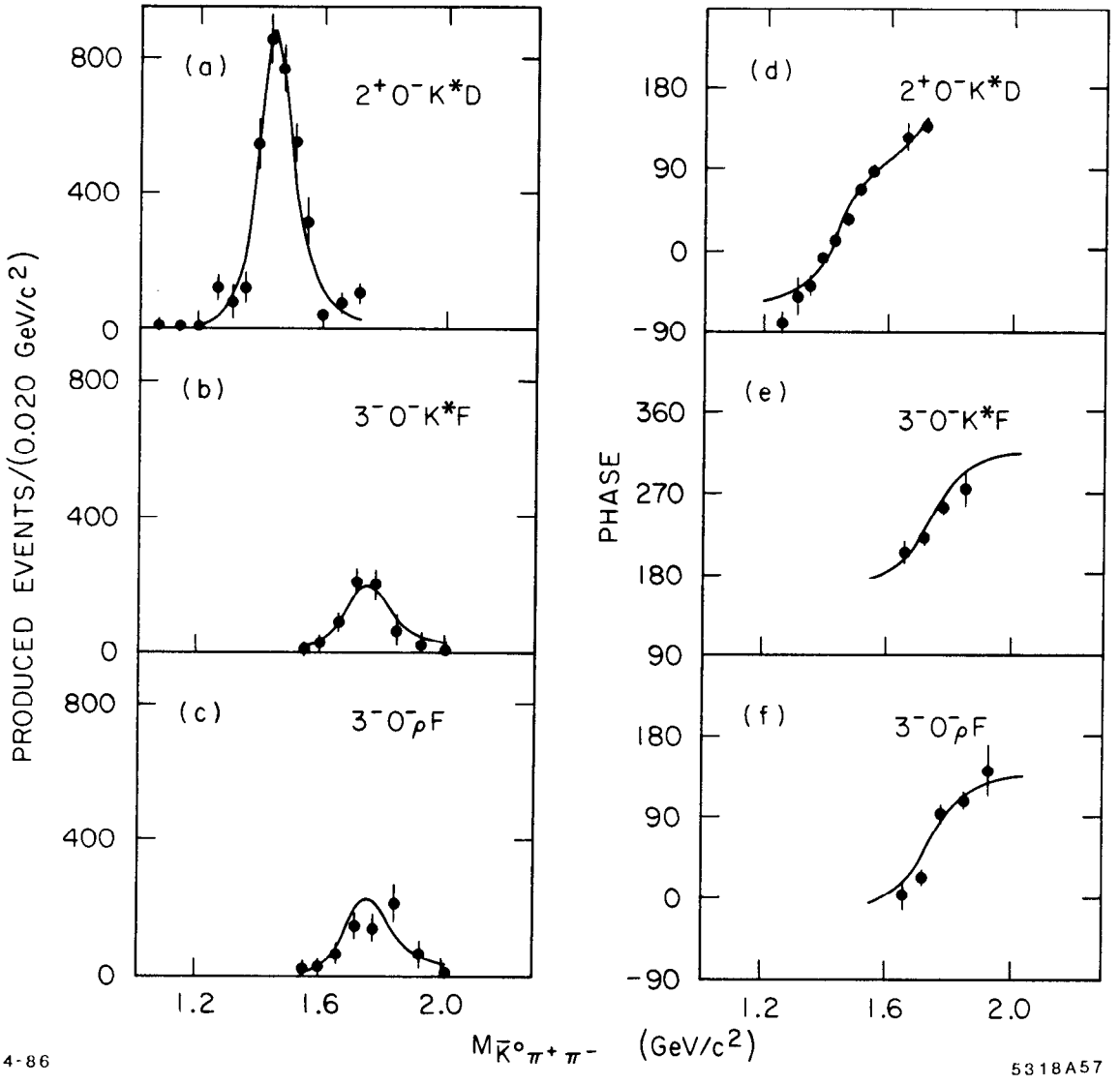
(a)
$2^+0^-K^*D$
(b)
$3^-0^-K^*F$
(c)
$3^-0^-\rho F$
(d)
$2^+0^-K^*D$
(e)
$3^-0^-K^*F$
(f)
$3^-0^-\rho F$
PRODUCED EVENTS/(0.020 GeV/c^2)
PHASE
$M_{\bar{K}^0\pi^+\pi^-}$ (GeV/c^2)
800
400
0
180
90
-90
360
270
1.2
1.6
2.0
4-86
5318A57

Fig. 5

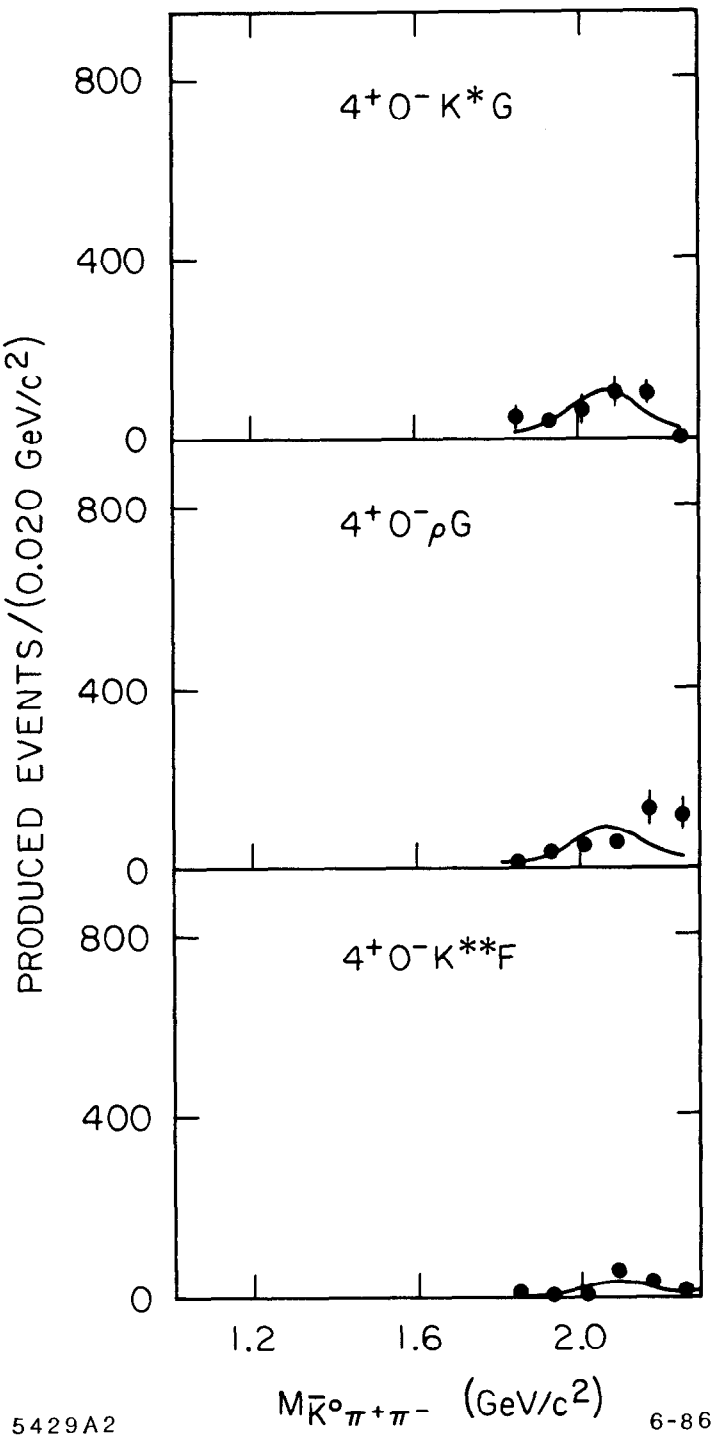
800
400
0
$4^+0^-K^*G$
800
400
0
$4^+0^-\rho G$
800
400
0
$4^+0^-K^{**}F$
PRODUCED EVENTS/(0.020 GeV/c^2)
1.2
1.6
2.0
$M_{\bar{K}^0\pi^+\pi^-}$ (GeV/c^2)
5429A2
6-86

Fig. 6

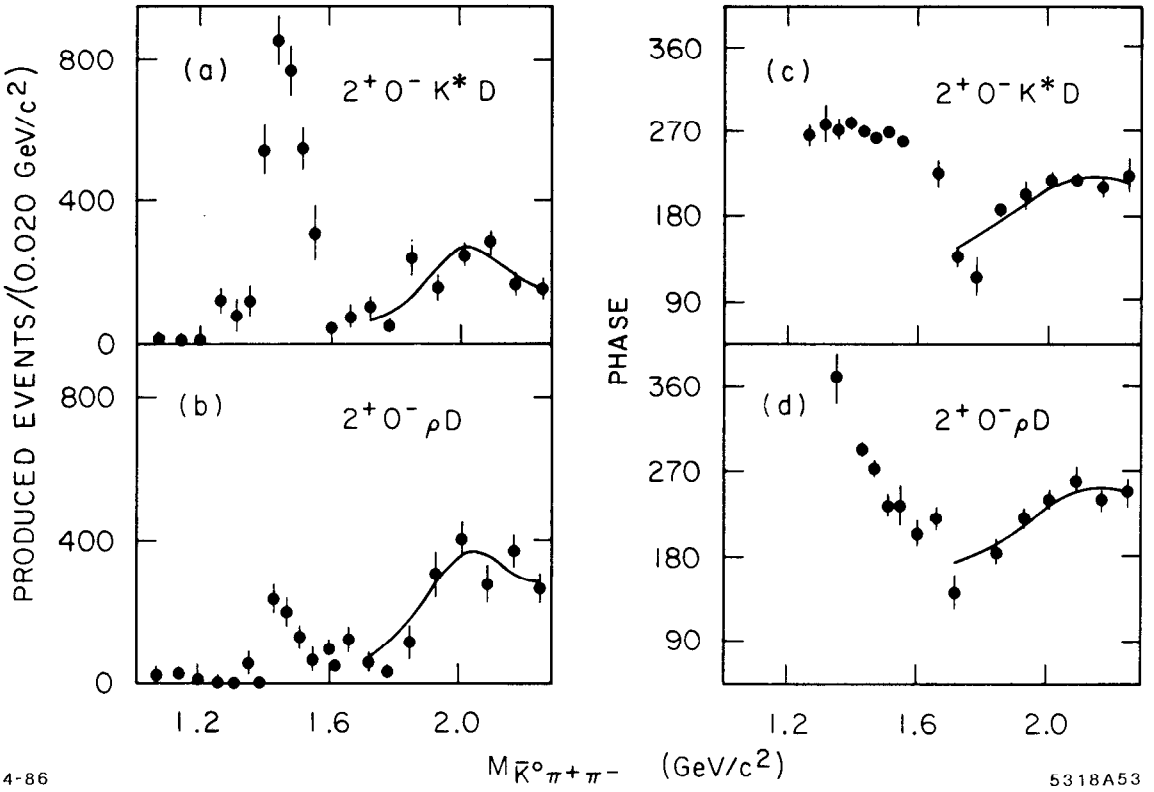
(a)
$2^+0^-K^*D$
(b)
$2^+0^-\rho D$
(c)
$2^+0^-K^*D$
(d)
$2^+0^-\rho D$
PRODUCED EVENTS/(0.020 GeV/c²)
PHASE
800
400
0
360
270
180
90
1.2
1.6
2.0
$M_{\bar{K}^0\pi^+\pi^-}$ (GeV/c²)
4-86
5318A53

Fig. 7

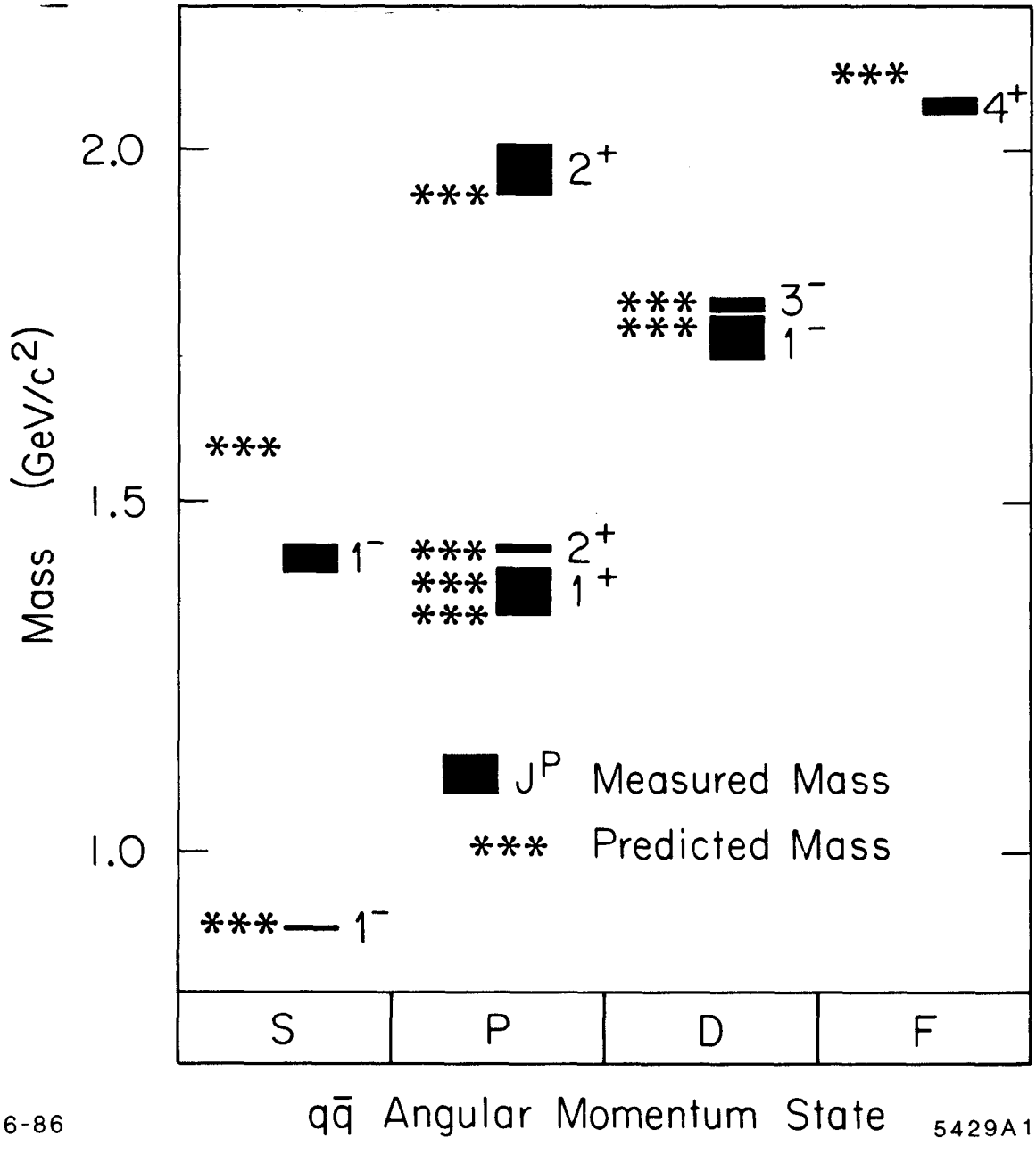
2.0
1.5
1.0
Mass (GeV/c²)
***
4+
2+
3−
1−
1+
J^P Measured Mass
*** Predicted Mass
S
P
D
F
qq̄ Angular Momentum State
6-86
5429A1

Fig. 8